ELSEVIER

Chemical Geology 208 (2004) 157–173

CHEMICAL GEOLOGY
INCLUDING
ISOTOPE GEOSCIENCE

www.elsevier.com/locate/chemgeo

Osmium isotope constraints on contrasting sources and prolonged melting in the Proterozoic upper mantle: evidence from ophiolitic Ru–Os sulfides and Ru–Os–Ir alloys

Kreshimir N. Malitch

Mineralogy and Petrology Group, Institute of Geological Sciences, University of Leoben, Peter Tunner Str. 5, A-8700 Leoben, Austria

Abstract

This study presents the first extensive data set of Os isotopic compositions of primary Ru–Os–Ir alloys and Ru–Os sulfides derived from two Neoproterozoic ophiolite-type ultramafic massifs (Kunar in Northern Taimyr, Russia, and Kraubath in Eastern Alps, Austria). The study employed a multi-technique approach and utilized a number of analytical techniques, including hydroseparation, electron microprobe analysis, negative thermal ionization mass-spectrometry (N-TIMS) and laser ablation attached to multiple collector-inductively coupled plasma-mass spectrometry (LA MC-ICP-MS). The results identify two different Os isotope sources (subchondritic and suprachondritic) for bedrock Ru–Os sulfides at Kraubath, whereas detrital Ru–Os–Ir alloys at Kunar are characterized by 'unradiogenic' $^{187}Os/^{188}Os$ values, indicative of a chondritic or subchondritic mantle source of platinum-group elements (PGE). The 'unradiogenic' $^{187}Os/^{188}Os$ values yield a very wide range of $^{187}Os/^{188}Os$ (0.1094 ± 0.0003 to 0.1241 ± 0.0004, $n = 19$, N-TIMS data), which is almost identical to the Os isotope composition of bedrock laurite, $(Ru,Os)S_2$, in podiform chromitite within an ophiolitic mantle section at Kraubath (0.11249 ± 0.00062 to 0.12437 ± 0.00051, $n = 17$, N-TIMS and LA MC-ICP-MS data). These results are consistent with a model in which a prolonged history of melting events of parent ultramafic source rocks took place in the oceanic upper mantle. In contrast, erlichmanite and laurite from banded chromitite within the transition zone at Kraubath show high $^{187}Os/^{188}Os$ (0.13080 to 0.13212) values, indicative of a suprachondritic source of PGE. This signature might be interpreted as either evidence of an enriched mantle source or an indication of a 'radiogenic' crustal component, which was introduced during a subduction-related event. The Os isotope results obtained support the conclusion that the Re–Os system, represented by PGM, has remained unchanged from the time of formation of the PGM until now, despite later thermal events, which occurred in the vicinity of ophiolite-type complexes.

Keywords: Laurite; Ru–Os–Ir alloy; Osmium isotopes; Chromitite; Ophiolite; Depleted upper mantle

1. Introduction

Os isotopes are considered an important tracer for understanding the evolution of highly siderophile elements in the upper mantle. Due to the progress of analytical techniques in recent years, the Re–Os system has been widely applied for evaluating distinct mantle sources and dating melting events in the mantle in different geological settings (Shirey and Walker, 1998; Hattori, 2002 and references sited therein). However, ambiguity in the use and interpre-

E-mail address: malitch@unileoben.ac.at (K.N. Malitch).

0009-2541/$ - see front matter © 2004 Elsevier B.V. All rights reserved.
doi:10.1016/j.chemgeo.2004.04.010

tation of whole rock Os isotope data has arisen from a number of recent mineral-scale Os isotopic studies (Burton et al., 1999; Alard et al., 2001, 2002 among others), which proved the existence of inter-mineral Os heterogeneity within individual samples. These studies showed that the primordial Os isotopic signature of base metal (BM) sulfides enclosed in silicate could easily be masked by highly radiogenic secondary BM sulfides, which cannot be estimated from whole rock Os isotopes alone. Furthermore, in situ laser ablation multiple collector-inductively coupled plasma-mass spectrometry (LA MC-ICP-MS) analyses of BM sulfides from abyssal and ophiolitic peridotites indicate a wide range of $^{187}Os/^{188}Os$ values from 0.1113 ± 0.0008 to 0.1382 ± 0.0014 (Alard et al., 2001). These results do not concur with the present day $^{187}Os/^{188}Os$ average estimates for either: (1) depleted mid-ocean ridge (MOR) mantle (DMM; 0.1246 ± 0.0014) deduced from the whole-rock Os isotopic compositions of abyssal peridotites (Snow and Reisberg, 1995); (2) primitive upper mantle (PUM; 0.1296 ± 0.0008) defined on the basis of whole-rock Os isotopic data for mantle xenoliths (Meisel et al., 2001); or (3) chondritic uniform reservoir (CHUR; 0.12863 ± 0.00046) as defined on the basis of the Os isotopic composition of ordinary chondrites (Chen et al., 1998). The origin of this heterogeneity is not well understood, especially regarding the timing of its development.

The depleted upper mantle, sampled from abyssal peridotites and the mantle sections of ophiolites, constitutes one of the most important geochemical reservoirs, which is not yet well constrained. In particular, several workers (Luck and Allègre, 1991; Walker et al., 1996; Tsuru et al., 2000) have demonstrated that Proterozoic and Phanerozoic ophiolites have broadly chondritic Os isotope signatures, consistent with derivation from a chondritic mantle. A recent attempt, based on ophiolitic chromite, defined an average Os isotopic composition of convecting mantle as 0.12809 (Walker et al., 2002). Chromite, one of the most resistant mantle minerals, is well protected from high-temperature serpentinization and low-temperature ocean-floor weathering in an ophiolite environment, and, thus, has been considered to represent initial $^{187}Os/^{188}Os$ values (Walker et al., 2002). It has been shown, however, that the Os budget of the mantle is mainly controlled by sulfide minerals and alloys (Hart and Ravizza, 1996; Burton et al., 1999). Therefore, Os-bearing platinum-group minerals (PGM) (i.e., Ru–Os sulfides and Ru–Os–Ir alloys) offer the most promise of avoiding ambiguity in the interpretation of Os isotopic results.

The advantage of the Re–Os system applied to mantle Os-bearing PGM is that these minerals contain osmium as a main or trace element in their crystal structures, and are essentially devoid of Re. This feature permits accurate initial Os isotope ratios to be determined, assuming that the Os isotopic compositions of Ru–Os–Ir alloys and Ru–Os sulfides have not changed after their formation and, therefore, reflects that of the source. A high resistance of the Os isotope system within Ru–Os–Ir alloys and Ru–Os sulfides to later thermal events has been demonstrated (Malitch et al., 2000, 2003a) for PGM samples from the Witwatersrand (South Africa) and Eastern Alps (Austria). Consequently, mantle Ru–Os–Ir alloys and Ru–Os sulfides encapsulated in chromite may contribute (1) to a better understanding of the $^{187}Os/^{188}Os$ evolution curve of the upper mantle and (2) to a more accurate interpretation of the processes leading to fractionation of Os isotopes in different mantle environments.

In the past, application of Os isotope studies of PGM from bedrock has been hampered by several factors. First, PGM are relatively small (usually less than 10–20 μm in diameter, grains more than 50–100 μm are rare). It is difficult, therefore, to liberate them from bedrock in significant amounts. A reliable technique to fully separate the PGM was lacking. However, separation from the matrix is needed to avoid uncertainties from excitation effects from host minerals (chromite, olivine, etc.) during Os isotope analysis. Developments in concentration techniques, including hydroseparation (Malitch et al., 2001, 2003b), and in Os isotope measurements (Creaser et al., 1991; Hirata et al., 1998; Kostoyanov et al., 2000; Junk, 2001, among others) now make it possible to obtain extensive quantitative data on relatively small PGM grains.

To demonstrate the high potential of Os isotopes, investigations were undertaken of compositionally different primary Ru–Os–Ir alloys and Ru–Os sulfides from two dunite–harzburgite massifs (Kunar, Russia, and Kraubath, Austria) of presumably Late Proterozoic age. A combined Os isotope study (negative thermal ionization mass-spectrome-

try, N-TIMS, and in situ LA MC-ICP-MS) was made of Os-rich minerals [Ru–Os–Ir alloy and erlichmanite, $(Os,Ru)S_2$] and PGM with Os contents as low as a few wt.% [laurite, $(Ru,Os)S_2$], which were characterized in advance by scanning electron microscopy and electron microprobe analysis (EMPA). The aim of this paper is to compare extensive data sets of Os isotopic compositions of detrital Ru–Os–Ir alloys at Kunar and bedrock Ru–Os sulfides from geologically and compositionally distinct chromitite samples at Kraubath in order to: (1) constrain the Os isotopic composition of the Late Proterozoic oceanic upper mantle; (2) determine the sources of PGE (e.g., chondritic, subchondritic, suprachondritic mantle); (3) specify the possible bedrock source of detrital PGM (e.g., mantle or crustal section of an ophiolite); and (4) provide age constraints on the formation of ultramafic protoliths hosting PGE-mineralization.

Frequently, Os isotope data have been presented without reporting the mineral chemistry of the Os–Ir alloys studied (e.g., Hirata et al., 1998; Meibom and Frei, 2002). In order to avoid this incompleteness, mineral compositions of Os-bearing PGM (e.g., Ru–Os–Ir alloys and laurite–erlichmanite series) are also presented.

2. Geology and sample location

2.1. Chelyuskin ophiolite

Ultramafic rocks of the Kunar massif (Fig. 1), which forms the northern part of the Chelyuskin ophiolite (Chelyuskin Peninsula at northeastern Taimyr, Russia), are composed mainly of metaperidotites (serpentinized harzburgites, dunites and associated chromitites). Metaperidotite bodies trend northeast for about 70 km and frequently are bordered by gabbroic rocks, narrow zones of serpentinite melange and greenschists (Zalyaleev and Bezzubtsev, 1975). Other rocks in the Chelyuskin ophiolite are tholeiitic basalts, dolerites of a dyke-sill complex and sheeted

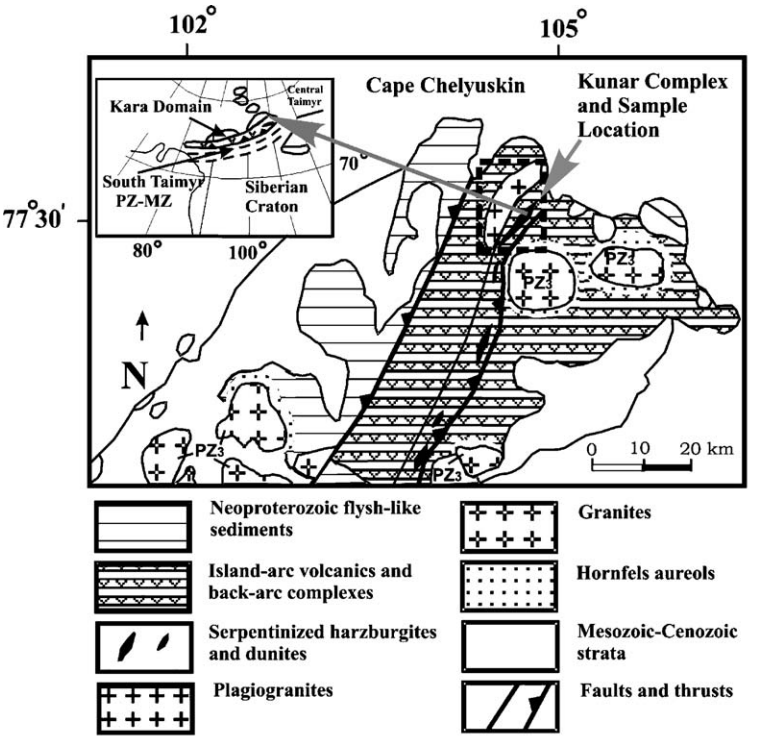

Fig. 1. Schematic geological map of northeastern Taimyr, modified after Vernikovsky and Vernikovskaya (2001).

plagiogranites. More detailed information on the geology of the Chelyuskin ophiolite, which forms part of the Neoproterozoic Central Taimyr Belt, has been summarized by Bezzubtsev et al. (1986) and Vernikovsky and Vernikovskaya (2001).

Geochronological information on the ultramafic rocks is lacking. However, U–Pb and Sm–Nd isotopic studies show that the plagiogranites of the Chelyuskin ophiolite formed between 850 and 740 Ma. It was subsequently metamorphosed to garnet amphibolite grade around 600 Ma, which is considered to be when the accretionary belt was emplaced onto the Arctic Siberian Craton passive margin (Vernikovsky and Vernikovskaya, 2001).

This study is based on 33 grains of Ru–Os–Ir alloy that range between 0.25 and 0.5 mm. These PGM were sampled from a gold production concentrate during prospecting of Jurassic and Quaternary placer deposits in the area of the Unga River. PGM occurrences are closely linked to the Kunar ultramafic Complex (Fig. 1). The Os isotope compositions of 19 Ru–Os–Ir alloy grains have been measured by N-TIMS.

2.2. Eastern Alpine ophiolite

The Kraubath dunite–harzburgite massif, situated within the Austrian Province of Styria, has been interpreted as a strongly metamorphosed Early Paleozoic or Precambrian dismembered ophiolite, emplaced during Variscan nappe tectonics (Neubauer et al., 1989). The Kraubath massif forms part of the Speik Complex, which rests tectonically on the Core Complex (Fig. 2), a Late Proterozoic to Early Paleozoic magmatic arc assemblage, which underwent a complex polyphase metamorphism between pre-Variscan and Alpine times (Faryad et al., 2002).

The Kraubath massif is composed of metamorphosed, foliated harzburgites and dunites dipping to the north with layers, lenses and stocks of coarse-grained orthopyroxenite. Recent attempts using whole rock analyses (Sm–Nd and Re–Os systematics) of ultramafic rocks of the Speik Complex, gave errorchron "ages" ranging from about ~780 Ma for the harzburgites to ~550 Ma for intrusive orthopyroxenites, respectively (Fig. 12 in Melcher et al., 2002). Suprachondritic $^{187}Os/^{188}Os$ values ($^{187}Os/^{188}Os_{(I)} = 0.178 \pm 0.003$) characteristic of orthopyroxenites are different from subchondritic $^{187}Os/^{188}Os$ values of the host harzburgites (0.12270–0.12578). On the basis of these results, a two-stage scenario has been proposed (Melcher et al., 2002): (1) partial melting of undepleted mantle during the Late Proterozoic resulted in formation of residual harzburgite in a mid-ocean ridge system or evolved back-arc basin; and (2) second-stage melting in a supra-subduction zone setting during the Early Cambrian, which led to the formation of a highly depleted residual mantle (harzburgites and dunites) and mantle melts, from which orthopyroxenites have been formed.

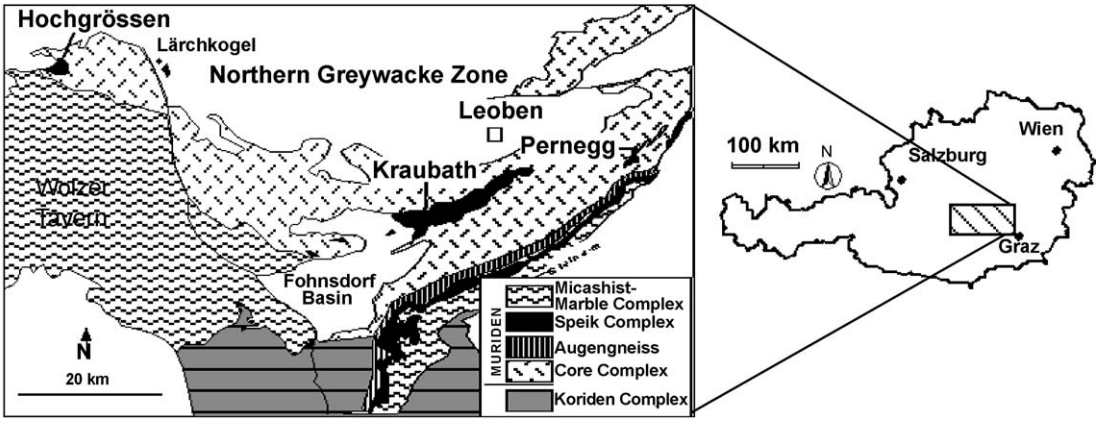

Fig. 2. Schematic geological map of Middle Austroalpine basement in central Styria showing location of the Kraubath, Hochgrösssen and Pernegg ultramafic massifs.

Numerous bodies of chromitite, generally less than 0.5 m in thickness, are exposed in the northern part of the Kraubath massif. The prevalent chromitite type occurs as deformed stringers and streaks of massive chromite not more than a few centimeters thick. According to the classification of Cassard et al. (1981), this type is considered to be typical podiform chromitite. Sample K 142, which is from a small outcrop in an abandoned open-pit chromite mine at Mitterberg (Sommergraben area), is representative of the podiform type from the mantle series rocks (Fig. 1 in Malitch et al., 2003b). The chemical composition of chromite varies in Cr# [100∗Cr/(Cr + Al)] from 80 to 86 and in Mg# [100∗Mg/(Mg + Fe^{2+})] from 44 to 50. Another, less abundant type of chromitite (i.e. sheet-like ore bodies, banded type) appears as layers of densely disseminated euhedral to subhedral chromite in a stratigraphically higher level of the massif, about 200 m north of the open-pit mines. Sample K 134, typical of this banded chromitite, is from a layer 5–25 cm thick, which is well exposed and can be traced for more than 30 m along dip (30–60° to the north) and (underground) for about 15 m along strike (Fig. 1 in Malitch et al., 2003b). The chemical composition of chromite varies in Cr# from 73 to 78 and in Mg# from 37 to 49. Based on geological, geochemical and mineralogical grounds, Malitch et al. (2003b) suggested that the banded chromitite from Kraubath is characteristic of the Moho transition zone, which divides mantle and crustal sections within an ophiolite.

The Os isotope compositions of 17 PGM grains, comprising laurite $(Ru,Os)S_2$ and erlichmanite $(Os,Ru)S_2$, from banded and podiform chromitites at Kraubath, have been measured by LA MC-ICP-MS and N-TIMS.

3. Analytical techniques

To constrain textural relationships of Ru–Os sulfides with the associated minerals, two samples of chromitite (K 142 and K 134) were first investigated optically. Ru–Os sulfides have been observed invariably as single and polyphase euhedral inclusions in chromite (Fig. 3a), thus revealing their primary signature. The chromitite samples (2.5 kg each) were subsequently disintegrated by gradual milling followed by removal and sieving of the fine fractions

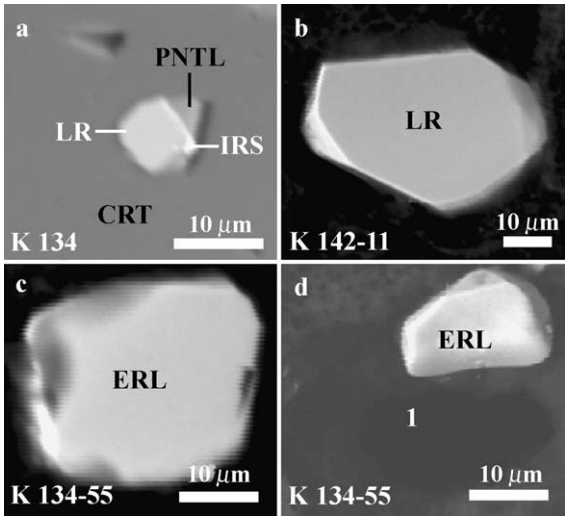

Fig. 3. Back scattered electron images of euhedral Ru–Os sulfide grains from distinct chromitites at Kraubath before (a–c) and after (d) laser ablation MC-ICP-MS. LR—laurite, ERL—erlichmanite, IRS—irarsite; PNTL—pentlandite, CRT—chromite; number 1 in black hole (d) indicate the area of the laser ablation MC-ICP-MS analysis, which corresponds to the same number in Table 4.

<37 and 37–100 μm. The heavy minerals (including PGM) of these two fractions were concentrated by a hydroseparation technique at NATI Research JSC, St. Petersburg, Russia, reaching concentration factors between 4×10^4 and 1×10^5 times. Details of this technique can be found on http://www.natires.com/. Each concentrate with PGM was then mounted in epoxy blocks and polished in separate sections for further detailed electron microprobe study (Fig. 3b,c). Detrital Ru–Os–Ir alloy grains at Kunar, represented by individual crystals and polymineral aggregates, were also mounted and polished, described and analyzed by electron microprobe analysis (EMPA) (Camscan-4 with energy-dispersive spectrometer Link-10 000 and wavelength spectrometer Microspec, JSC Mekhanobr-Analyt, St.-Petersburg, Russia and ARL-SEMQ microprobe with four wavelength-dispersive spectrometers (WDS) and equipped with a LINK energy dispersive analyser, Institute of Geological Sciences, University of Leoben, Austria). Quantitative WDS analyses were performed at 25 kV accelerating voltage and 20 nA sample current, with a beam diameter of about 1 μm. The following X-ray lines and standards were used: RuLα, RhLα, PdLβ, OsMα, ReLα, IrLα, PtLα, NiKα (all native element

standards); FeKα, CuKα, SKα (all chalcopyrite); AsLα (sperrylite). Corrections were performed for the interferences involving Ru–Rh, Ru–Pd and Ir–Cu. A total of 191 quantitative analyses were made on Ru–Os–Ir alloys and Ru–Os sulfides.

After electron microprobe analysis, the 15 grains of Ru–Os sulfides from geologically and compositionally distinct chromitites at Kraubath (e.g., podiform type from an ophiolite mantle section, sample K 142, and banded type from an ophiolitic transition zone, sample K 134) were investigated by LA MC-ICP-MS at the Technical University of Mining and Metallurgy (Institute of Archaeometry), Freiberg, Germany. Finally, 2 grains of laurite from podiform chromitite at Kraubath and 19 detrital grains of Ru–Os–Ir alloy derived from the Kunar Complex were removed from the resin and the osmium isotope ratios were determined in the individual PGM by N-TIMS at the Department of Isotope Geology, All-Russia Geological Research Institute (VSEGEI), St. Petersburg, Russia.

LA measurements were performed with a Microprobe II LA device (Thermo Elemental, Nd:YAG laser, 266 nm wavelength) and an AXIOM MC-ICP-MS (Thermo Elemental Axiom, multicollector version featuring 9 Faraday cup detectors operated at a mass resolution of 400). The ICP-MS was tuned using a desolvating nebulizer (MCN 6000, CETAC), a solution of 33 μg/l Re, 330 μg/l Os, and 330 μg/l Ir in 2% nitric acid, a nebulizer flow of 0.8 l/min Ar, and a radio frequency (RF) forward power of 1330 W. Helium was used as an ablation chamber gas with a flow of 85 ml/min that has minimised dead volume. The air capacitor of the ICP-MS was optimised to obtain a RF reflected power of 12 to 18 W with this He addition to the plasma gas. The MC set-up, and corrections for Re and W contents, were checked with combined laser ablation analyses of members of the ferberite–hübnerite series and the aerosol generated by the desolvating nebulizer, as described by Junk (2001).

LA spots of 5 to 30 μm were used with a scan field that was adapted to the size of each sampling area (Fig. 3d), a laser shot frequency of 20 Hz, and an energy output of up to 0.5 mJ. The aerosols generated by LA were transported by a gas stream to the MC-ICP-MS. Nine signals were measured simultaneously at *m/z* 183 (W), 184 (W + Os), 185 (Re), 186 (W + Os), 187 (Re + Os), 188 (Os), 189 (Os), 191 (Ir) and 193 (Ir) using the multichannel collector of the ICP-MS. The mass bias was corrected using an exponential fractionation law and the $^{188}Os/^{189}Os$ ratio. The validity of the fixed ^{188}Os /^{189}Os ratio was tested by a mass bias correction using the $^{191}Ir/^{193}Ir$ ratio, as described by Junk (2001). Isobaric interferences were very rare and were thus corrected using the natural abundances of Re or W. For the reported values, no significant contribution of possible error sources was detected. The abundances used for the calculations were taken from Rosman and Taylor (1998) (at.%, $^{184}Os = 0.02$, $^{186}Os = 1.59$, $^{188}Os = 13.24$, $^{189}Os = 16.15$, $^{190}Os = 26.26$ and $^{192}Os = 40.78$). The isotope ratios are reported with experimental uncertainties taking into account the contributions of the Faraday cup efficiencies, the normalization value for mass bias corrections using $^{188}Os/^{189}Os$ (Rosman and Taylor, 1998), interference corrections, the signal noise, and the within-run standard deviations. Repeated analyses ($n = 26$) of a natural Os–Ir alloy (Table 4, an. 20), which has been used to check the validity of the LA MC-ICP-MS measurements, yield $^{187}Os/^{188}Os = 0.12162 \pm 0.00020$ (2 sigma uncertainty). Furthermore, it has been shown (Malitch et al., 2002) that the Os isotopic composition of Os–Ir alloy (i.e., $Os_{0.89}Ir_{0.11}$) from the Bor-Uryah massif measured by LA MC-ICP-MS ($^{187}Os/^{188}Os = 0.12396 \pm 0.00013$) is in accordance with N-TIMS analysis of the same sample ($^{187}Os/^{188}Os = 0.1240 \pm 0.0002$). A more detailed description of the LA MC-ICP-MS technique is given by Junk (2001) and Malitch et al. (2003a).

To measure the Os isotopic composition of PGM by N-TIMS, a modernized MI-1320 instrument (Kostoyanov et al., 2000) was used. Osmium isotopes were determined by one-tape detection of negative OsO_3^- ions formed on the cathode surface at temperatures of 700–1400 °C. The method allows the analysis of individual PGM weighing as little as 10^{-7} g and containing more than 10 wt.% of osmium. The sizes of individual PGM grains were sufficient to maintain the signal from one of the most abundant Os isotopes (^{190}Os) at 10^{-13}–10^{-14} Å for several hours. Measured isotope ratios were normalized by taking into account both isobar and mass-fractionation effects. The mass-fractionation effect was considered to be exponentially related to the detected ion mass. Precision of the osmium isotope determinations, based on

the reproducibility of isotope ratios in one series of repeated runs, was found to be 0.3%. During the measurements of the laboratory standard, composed of grains of OsO_2, no systematic errors were found. The $^{190}Os/^{188}Os$ value of independent runs of the laboratory standard (1.9837 ± 0.0004, Kostoyanov et al., 2000) was within the range of random errors for the $^{190}Os/^{188}Os$ value of the osmium-DTM-standard measured by Finnigan MAT-262 (1.98378 ± 0.00002, Tuttas). Further details on the method and analytical precisions are given in Kostoyanov et al. (2000), Malitch et al. (2000) and Hattori (2002).

4. PGE mineralogy

The compositions of Ru–Os–Ir alloys and Ru–Os sulfides along with their morphological features are presented in Figs. 3 and 4. The chemical compositions of the PGM are given in Tables 1 and 2.

4.1. Chelyuskin ophiolite

At Kunar, a diversity of alloys of the Ru–Os–Ir system have been observed. According to the nomenclature of Harris and Cabri (1991), they comprise

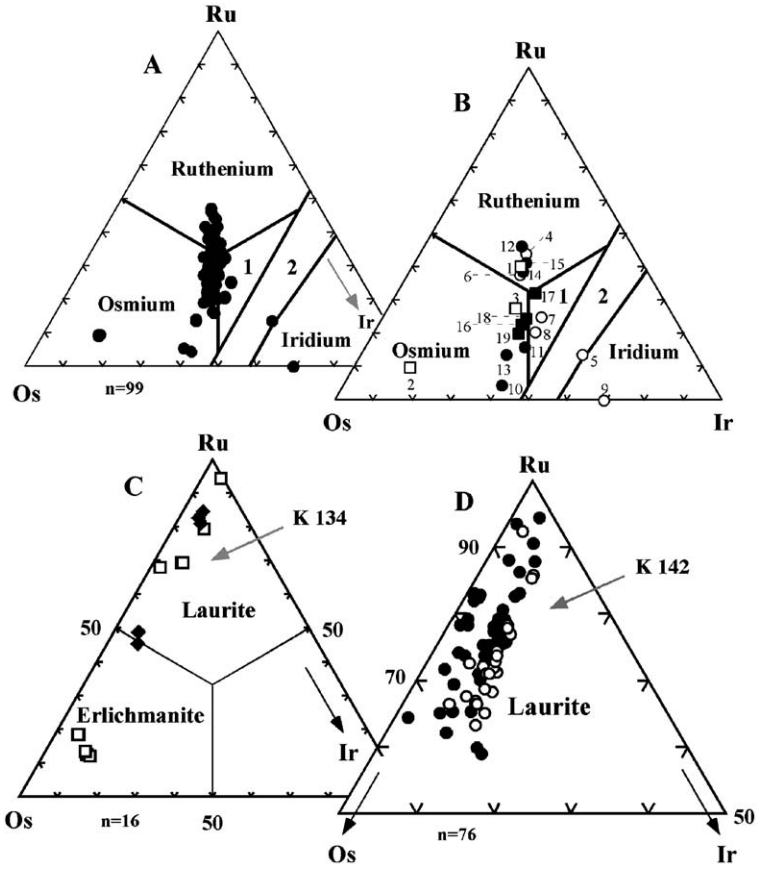

Fig. 4. Composition of detrital Ru–Os–Ir alloys at Kunar (A, B) and Ru–Os sulfides from banded (K 134) and podiform (K 142) chromitites at Kraubath (C, D) in the ternary diagram Ru–Os–Ir, at.%. Fields 1 and 2—rutheniridosmine and miscibility gap, respectively. (A) shows 99 electron microprobe analyses for 33 PGM grains studied. (B) Ru–Os–Ir alloys measured by N-TIMS, subdivided according to their Os isotope composition: open squares refer to PGM with $^{187}Os/^{188}Os$ less than 0.1202, open circles—$^{187}Os/^{188}Os = 0.1214–0.1221$, filled circles—$^{187}Os/^{188}Os = 0.1225–1231$, filled squares—$^{187}Os/^{188}Os = 0.1237–0.1241$. (C) Open squares and closed diamonds refer to single and polyphase Ru–Os sulfides from banded chromitite, respectively. (D) Open and closed circles refer to single and polyphase laurite from podiform chromitite, respectively. Numbers 1–19 correspond to the same numbers in Tables 1 and 3.

Table 1
Representative electron microprobe analyses (WDS) of Ru–Os–Ir alloys derived from the Kunar ultramafic massif, Russia

No.	1	2	3	4	5	6	7	8	9	10	11	12	13	14	15	16	17	18	19
Sample	1-4	2-3	3-5	2-4	5-3	6-5	3-3	4-5	2-5	5-2	4-3	4-2	4-1	64-2	2-1	3-4	1-1	4-4	6-7
Mineral[a]	RIO	Ru	Os	Os	Ir	Ru	RIO	RIO	Ir	Os	Os	Ru	Os	Ru	Ru	Os	RIO	Os	Os
wt.%																			
Fe	0.00	0.00	0.00	0.00	0.33	0.00	0.00	0.55	0.34	0.00	0.59	0.00	0.00	0.23	0.00	0.00	0.32	0.00	0.00
Ni	0.00	0.00	0.00	0.00	0.00	0.00	0.00	0.00	0.00	0.00	0.00	0.00	0.00	0.14	0.00	0.00	0.00	0.00	0.00
Ru	24.35	5.15	16.07	29.08	6.81	22.67	14.57	11.82	0.00	2.35	9.12	29.53	7.62	23.60	27.16	12.90	19.84	14.69	11.46
Rh	0.00	0.00	0.00	0.00	0.39	0.00	0.00	0.00	0.00	0.00	0.00	0.00	0.00	0.00	0.00	0.00	0.00	0.00	0.00
Os	36.59	78.97	43.89	35.93	27.94	37.75	37.75	41.94	30.23	55.42	45.77	34.78	51.57	36.99	36.85	43.89	37.17	42.80	46.78
Ir	32.66	15.26	36.55	33.92	54.73	32.75	44.83	45.83	69.35	41.59	43.92	29.96	39.85	33.84	35.55	39.96	40.99	41.87	40.83
Pt	5.55	0.00	2.93	0.00	8.86	5.78	2.75	0.00	0.00	0.00	0.00	5.07	0.00	4.24	0.00	2.27	0.70	0.00	0.00
Total	99.15	99.38	99.44	98.93	99.06	98.95	99.90	100.14	99.92	99.36	99.40	99.34	99.04	99.04	99.56	99.02	99.02	99.36	99.07
at.%																			
Fe	0.00	0.00	0.00	0.00	1.07	0.00	0.00	1.68	1.16	0.00	1.85	0.00	0.00	0.65	0.00	0.00	0.93	0.00	0.00
Ni	0.00	0.00	0.00	0.00	0.00	0.00	0.00	0.00	0.00	0.00	0.00	0.00	0.00	0.38	0.00	0.00	0.00	0.00	0.00
Os	38.14	9.34	26.73	44.06	12.16	36.01	24.44	19.97	0.00	4.38	15.83	44.47	13.61	36.93	41.50	22.09	31.96	24.71	19.83
Rh	0.00	0.00	0.00	0.00	0.69	0.00	0.00	0.00	0.00	0.00	0.00	0.00	0.00	0.00	0.00	0.00	0.00	0.00	0.00
Ru	30.46	76.11	38.79	28.92	26.51	31.87	33.64	37.65	30.23	54.87	42.22	27.84	48.96	30.76	29.93	39.93	31.83	38.26	43.02
Ir	26.90	14.55	31.96	27.02	51.37	27.36	39.53	40.70	68.61	40.75	40.10	23.73	37.43	27.84	28.57	35.97	34.70	37.03	37.15
Pt	4.50	0.00	2.52	0.00	8.20	4.76	2.39	0.00	0.00	0.00	0.00	3.96	0.00	3.44	0.00	2.01	0.58	0.00	0.00

[a] RIO = rutheniridosmine, Os = osmium, Ru = ruthenium and Ir = iridium; concentrations of Pd, Re and Cu are below the detection limit of EMPA.

osmium, ruthenium, rutheniridosmine and iridium (Table 1 and Fig. 4A). Most of the PGM grains are monophase (28 cases). Five polymineralic grains (samples 1-2, 3-4, 3-5, 5-2 and 6-1) are dominated by various IPGE (Os, Ir, and Ru) alloys, with minor amounts of one or several other PGM (e.g., Pt–Fe alloy close to Pt_3Fe, chengdeite Ir_3Fe, cuproiridsite $CuIr_2S_4$, laurite $(Ru,Os)S_2$, unnamed Os–Ir sulfide $(Os,Ir)S_2$, irarsite IrAsS and moncheite $PtTe_2$). PGM are dominated by osmium, followed by ruthenium, rutheniridosmine and iridium (Fig. 4A). Such diversity of IPGE alloys is not unusual in ophiolite-type complexes (Cabri et al., 1996). The trend towards ruthenium in the mineral compositions (Fig. 4A,B) is, according to Bird and Bassett (1980), due to the formation of these minerals under high-pressure mantle conditions.

4.2. Eastern Alpine ophiolite

Whole-rock PGE concentrations and the PGM assemblages of two chromitite samples (K 134 and K 142) from the Kraubath massif have been studied in detail by Malitch et al. (2003b) and are, thus, only briefly summarized here. The podiform chromitite (sample K 142) displays a negatively sloped chondrite-normalized PGE pattern typical of ophiolitic-podiform chromitite, whereas the banded chromitite is enriched in Pt and Pd (sample K 134). It is noteworthy that PGE mineralogy is in good accordance with PGE distribution patterns of both chromitites investigated (Malitch et al., 2003b).

Ru–Os sulfides (laurite, $(Ru,Os)S_2$ and erlichmanite, $(Os,Ru)S_2$) occur as (a) single grains and (b) polyphase assemblages (Fig. 3). Ru–Os sulfides (Ru number $[100*Ru_{at.\%}/(Ru+Os)_{at.\%}]$ varies from 97 to 14) are dominated by Ru-rich sulfide (laurite), whereas Os-rich sulfide (erlichmanite) is less common (Table 2, Fig. 4C,D). Ru–Os sulfides from banded chromitite display a larger variation in terms of the Ru number (from 89 to 14); Ru–Os sulfides from podiform chromitite have Ru numbers ranging from 97 to 66 only (Table 2 and Fig. 4C,D). The composition of members of the laurite–erlichmanite series, when plotted on the Ru–Os–Ir ternary diagram (Fig. 4C,D), shows common Ru substitution for Os. Laurite usually carries moderate concentrations of both Ir and Rh, whereas erlichmanite con-

Table 2
Representative electron microprobe analyses (WDS) of Ru–Os sulfides from distinct chromitites at Kraubath, Eastern Alps, Austria

Sample	134-55	134-66	142/100-11	142/100-10	142-20	142-15	142-14	142-10	142-95	142-103
Mineral	ERL[a]	Laurite	Laurite	Laurite	Laurite	Laurite	Laurite	Laurite	Laurite	Laurite
wt.%										
S	26.72	34.98	34.79	34.59	33.66	33.91	33.65	33.80	34.52	34.48
Fe	0.22	0.23	0.00	0.19	0.29	0.21	0.29	0.00	0.16	0.28
Ru	5.31	45.23	39.80	39.98	40.42	38.57	38.71	39.50	42.51	42.81
Rh	0.00	0.00	1.36	1.42	0.00	0.00	0.00	0.00	1.95	0.00
Os	59.52	12.80	15.88	16.74	19.61	21.59	18.61	19.82	14.01	18.92
Ir	8.01	5.89	8.43	7.53	5.67	5.61	8.41	6.98	6.53	2.66
Total	99.78	99.13	100.26	100.45	99.65	99.89	99.67	100.10	99.52	99.15
at.%										
S	66.86	66.50	67.00	66.65	66.13	66.70	66.46	66.49	66.19	66.50
Fe	0.32	0.25	0.00	0.21	0.33	0.24	0.33	0.00	0.18	0.31
Ru	4.21	27.28	24.31	24.43	25.19	24.06	24.25	24.65	25.85	26.19
Rh	0.00	0.00	0.82	0.85	0.00	0.00	0.00	0.00	1.16	0.00
Os	25.27	4.10	5.16	5.44	6.49	7.16	6.20	6.57	4.53	6.15
Ir	3.34	1.87	2.71	2.42	1.86	1.84	2.77	2.29	2.09	0.86

[a] ERL = erlichmanite, concentrations of Pt, Pd, Re, Ni, Cu and As are below the detection limit of EMPA.

tains notable concentrations of Ru and Ir only (Table 2). The compositions of the Ru–Os sulfides span most of the wide compositional range of the laurite–erlichmanite series of mantle-hosted chromitites (Melcher et al., 1997; Garuti et al., 1999, and references cited therein).

5. Osmium isotope data

The $^{187}Os/^{188}Os$ values along with calculated model ages of detrital PGM at Kunar and bedrock PGM at Kraubath are presented in Tables 3 and 4 and Fig. 5. Since the concentration of Re in all samples is less than the detection limit by EMPA (0.05 wt.%), the isotopic effect of ^{187}Re in situ radioactive decay can be considered negligible when discussing the analytical data. Hence, the value of $^{187}Os/^{188}Os$ in the PGM under discussion corresponds to that in the source of the ore material at the time of PGM formation.

5.1. Chelyuskin ophiolite

The $^{187}Os/^{188}Os$ ratio in the investigated PGM ranges from 0.1094 ± 0.0004 to 0.1241 ± 0.0004 (Table 3). Excluding three PGM grains (samples 1-4, 2-3 and 3-5, Table 3, Fig. 4) with the lowest $^{187}Os/^{188}Os$ values (< 0.1203), at least three PGM groups can be estimated, with average $^{187}Os/^{188}Os$ values of 0.1218 ± 0.0003 ($n = 5$), 0.1230 ± 0.0003 ($n = 7$) and 0.1239 ± 0.0003 ($n = 4$), respectively (Table 3, uncertainties are within the 95% confidence level). No correlation between chemical composition and isotope content of the samples was observed (Tables 1 and 3; Fig. 4B). Osmium isotope ratios of optically homogeneous PGM crystals are similar to those of polyphase PGM grains. 'Unradiogenic' $^{187}Os/^{188}Os$ values of IPGE alloys indicate that the Re–Os system in PGM (i.e., osmium, ruthenium, rutheniridosmine and iridium) has remained unchanged, despite a secondary metamorphic overprint. The stability of the Os isotope system at the mineral level has also been demonstrated for detrital 3.0–3.2-Ga-old Ru–Os–Ir alloys from the Evander goldfield at Witwatersrand, South Africa (Malitch et al., 2000).

Since the $^{187}Os/^{188}Os$ values in all analyzed Ru–Os–Ir alloys do not exceed the value of the average present-day chondriric uniform reservoir (0.12863 ± 0.00046, Chen et al., 1998), a model (mantle-derived) age can be calculated according to the method of Allègre and Luck (1980). In order to calculate model Re–Os ages of PGM, the $^{187}Os/^{188}Os$ evolution curve of the CHUR has to be known and constrained by initial and present-day $^{187}Os/^{188}Os$ values. In this study, I am using the initial and present-day $^{187}Os/^{188}Os$ values (0.0953 ± 0.0013 and 0.12863 ± 0.00046, respective-

Table 3
N-TIMS Os isotopic composition and calculated model ages of detrital Ru–Os–Ir alloys from the Chelyuskin ophiolite, Russia

Analysis	Sample	Mineral, Ru number	Atomic proportions	Pt/Os	$^{187}Os/^{188}Os$	$T_{(ch)}$, Ga
1	1-4	Ruthenium, 56	(Ru, Os, Ir)	0.15	0.1094 (4)	2.669
2	2-3	Osmium, 11	(Os, Ir)	0.00	0.1189 (3)	1.365
3	3-5	Osmium, 41	(Os, Ir, Ru)	0.07	0.1202 (3)	1.184
4	2-4	Ruthenium, 60	(Ru, Os, Ir)	0.00	0.1214 (3)	1.017
5	5-3	Iridium, 31	(Ir, Os, Ru)	0.32	0.1217 (3)	0.975
6	6-5	Ruthenium, 53	(Ru, Os, Ir)	0.15	0.1217 (3)	0.975
7	3-3	RIO*, 42	(Ir, Os, Ru)	0.07	0.1219 (3)	0.947
8	4-5	RIO*, 35	(Ir, Os, Ru)	0.00	0.1221 (3)	0.919
Average 1 (an. 4 to 8)		IPGE alloys ($n=5$)			0.1218 (3)	0.961
9	2-5	Iridium, 0	(Ir, Os)	0.00	0.1225 (3)	0.864
10	5-2	Osmium, 7	(Os, Ir)	0.00	0.1229 (3)	0.808
11	4-3	Osmium, 27	(Os, Ir, Ru)	0.00	0.1229 (3)	0.808
12	4-2	Ruthenium, 62	(Ru, Os, Ir)	0.15	0.1230 (3)	0.794
13	4-1	Osmium, 22	(Os, Ir, Ru)	0.00	0.1231 (3)	0.780
14	64-2	Ruthenium, 55	(Ru, Os, Ir)	0.11	0.1231 (4)	0.780
15	2-1	Ruthenium, 58	(Ru, Os, Ir)	0.00	0.1231 (4)	0.780
Average 2 (an. 9 to 15)		IPGE alloys ($n=7$)			0.1230 (4)	0.794
16	3-4	Osmium, 36	(Os, Ir, Ru)	0.05	0.1237 (3)	0.696
17	1-1	RIO*, 50	(Ir, Ru, Os)	0.02	0.1238 (3)	0.681
18	4-4	Osmium, 39	(Os, Ir, Ru)	0.00	0.1241 (3)	0.639
19	6-7	Osmium, 32	(Os, Ir, Ru)	0.00	0.1241 (4)	0.639
Average 3 (an. 16 to 19)		IPGE alloys ($n=4$)			0.1239 (4)	0.667

RIO*—rutheniridosmine; Ru number $=100*Ru_{at.\%}/(Ru+Os)_{at.\%}$; $^{187}Os/^{188}Os$ normalized to $^{190}Os/^{188}Os=1.98379$ (Tuttas, 1992); numbers in parentheses are 2σ uncertainty in the last decimal places of $^{187}Os/^{188}Os$ ratios using machine error; model ages were calculated with values estimated by Chen et al. (1998) and a ^{187}Re decay constant of $\lambda=1.666\times10^{11}$ year^{-1} (Smoliar et al., 1996).

ly) along with the present day $^{187}Re/^{188}Os$ value (0.423 ± 0.007) as estimated by Chen et al. (1998). Alternative $^{187}Os/^{188}Os$ values for the present-day mantle, in widespread use for calculation of model ages, are 0.12736 (Yin et al., 1996), 0.1270 (Shirey and Walker, 1998) and 0.1296 ± 0.0008 (Meisel et al., 2001), where $^{187}Re/^{188}Os$ is taken as 0.40186 (Shirey and Walker, 1998). Calculations using the first two $^{187}Os/^{188}Os$ estimates would result in model ages that are approximately 0.15–0.2 Ga younger. If the $^{187}Os/^{188}Os$ value of PUM is used, the model ages of PGM are approximately 0.2 Ga older. However, as is clear from recent studies of BM sulfides (Alard et al., 2001, 2002), the latter estimate cannot be considered a valid proxy material for mantle sulfides.

Model age estimates for the formation of the ultramafic protoliths, based on osmium isotopic compositions of Ru–Os–Ir alloys, fall in the range of 2669–639 Ma (Table 3, N-TIMS study, $n=19$). The three PGM groups mentioned above have average model ages of 0.961 ± 0.045, 0.794 ± 0.045 and 0.667 ± 0.060 Ga, respectively (Table 3).

5.2. Eastern Alpine ophiolite

Os isotope measurements of Ru–Os sulfides from banded chromitite at Kraubath (i.e., erlichmanite, K134-55, Fig. 3c,d, and laurite, K 134-66) yield the highest $^{187}Os/^{188}Os$ (0.13080 ± 0.00011 to 0.13212 ± 0.00065, respectively) values, compared to the 'unradiogenic' $^{187}Os/^{188}Os$ values of detrital Ru–Os–Ir alloys at Kunar and laurite from podiform chromitite at Kraubath (Tables 3 and 4; Fig. 5). Indeed, the $^{187}Os/^{188}Os$ ratio in laurite from Kraubath varies between 0.11249 ± 0.00062 and 0.12437 ± 0.00051 (Table 4, Fig. 5). The dispersion of $^{187}Os/^{188}Os$ values in grains of laurite from podiform chromitite exceeds the analytical uncertainty. Therefore, isotopic variation among the majority of laurites is significant and is very similar to that of Ru–Os–Ir alloys at Kunar. Furthermore, the $^{187}Os/^{188}Os$ values of PGM at Kraubath are similar to those from podiform chromitite at Hochgrössen (Malitch et al., 2003a), another mantle relict in the Eastern Alps (Fig. 2). The wide range of $^{187}Os/^{188}Os$ values of laurite from the Kraubath massif in this

study results in $^{187}Os/^{188}Os$ model ages in the range of 2248–601 Ma (Table 4, $n=15$).

6. Discussion

Os isotope studies of PGM have been mainly restricted to placer occurrences derived from Phanerozoic ophiolite- and zoned-type complexes (Hattori and Hart, 1991; Malitch, 1999; Hattori, 2002 and references cited therein). The Os isotope data on bedrock PGM from an ophiolitic environment are scarce. Three analyses of laurites measured by MIT-Harvard-Brown Cameca 3f ion microprobe have been reported by Hattori et al. (1992). Other Os isotopic analyses of laurites have been presented by Walker et al. (1996), Ohnenstetter et al. (1999) and Malitch et al. (2003a). Os isotopic data on Os–Ir alloy (Os, Ir) and ruarsite (Ru,Os)AsS have been reported by Rudashevsky et al. (1999) and Malitch et al. (2003a), respectively. The present study provides new constraints on the osmium isotopic composition of the oceanic upper mantle based on an extensive data set of (1) detrital Ru–Os–Ir alloys closely linked to the Kunar massif (Chelyuskin Peninsula at northeastern Taimyr, Russia) and (2) bedrock Ru–Os sulfides from well-constrained stratigraphic positions within the ultramafic sequences of the Kraubath massif (Eastern Alps, Austria).

Table 4
Os isotopic composition and calculated model ages of bedrock Ru–Os sulfides from the Eastern Alpine ophiolite, Austria

Analysis	Sample	Mineral, Ru number	Os, wt.%	$^{187}Os/^{188}Os$	$T_{(ch)}$, Ga
Banded chromitite at Kraubath					
1	134-55	ERL*, 14, Fig. 3c,d	59.52	0.13080 (11)	
2	134-66	Laurite, 87	12.80	0.13212 (65)	
Podiform chromitite at Kraubath					
3	142-21	Laurite, 85	14.09	0.11249 (62)	2.248
4	142/100-11	Laurite, 83, Fig. 3b	15.88	0.1158 (4)	1.794
5	142/100-10	Laurite, 82	16.74	0.1162 (4)	1.738
6	142-20	Laurite, 80	19.61	0.12027 (71)	1.174
7	142-15	Laurite, 77	21.59	0.12044 (35)	1.151
8	142/100-9	Laurite, 77	21.77	0.12077 (71)	1.105
9	142-14	Laurite, 80	18.61	0.12133 (76)	1.027
10	142/100-6	Laurite, 84	15.89	0.12180 (64)	0.961
11	142-101	Laurite, 88	13.20	0.12292 (70)	0.805
12	142-10	Laurite, 79	19.82	0.12328 (29)	0.754
13	142-70	Laurite, 82	15.42	0.12334 (35)	0.745
14	142-100	Laurite, 83	16.01	0.12337 (51)	0.742
15	142-95	Laurite, 85	14.01	0.12357 (46)	0.714
16	142-106	Laurite, 97	1.92	0.12395 (33)	0.660
17	142-103	Laurite, 80	18.92	0.12437 (51)	0.601
Podiform chromitite at Hochgrössen (Malitch et al., 2003a)					
18	71-1	Laurite, 80	19.40	0.11940 (52)	1.296
19	71-2	Laurite, 63	30.90	0.12392 (82)	0.665
Placer deposits near Nizhny Tagil area (Russia)					
20	38331	Os–Ir alloy	–	0.12162 (20)	

ERL*—erlichmanite; an. 1–3, 6-20—LA MC-ICP-MS data; an. 4 and 5 N-TIMS data; Ru number = $100*Ru_{at.\%}/(Ru+Os)_{at.\%}$; numbers in parentheses are 2σ uncertainty in the last decimal places of $^{187}Os/^{188}Os$ ratios; model ages were calculated with values estimated by Chen et al. (1998) and a ^{187}Re decay constant of $\lambda = 1.666\times10^{-11}$ year^{-1} (Smoliar et al., 1996); $^{187}Os/^{188}Os$ reproducibility < 0.02% (2 S.D.) as determined from natural Os–Ir alloy measurement (sample no. 38331, Laggerstättenkunliche Sammlung, TU Bergakademie Freiberg); 20—average of 26 measurements from 21 March to 01 July 2001.

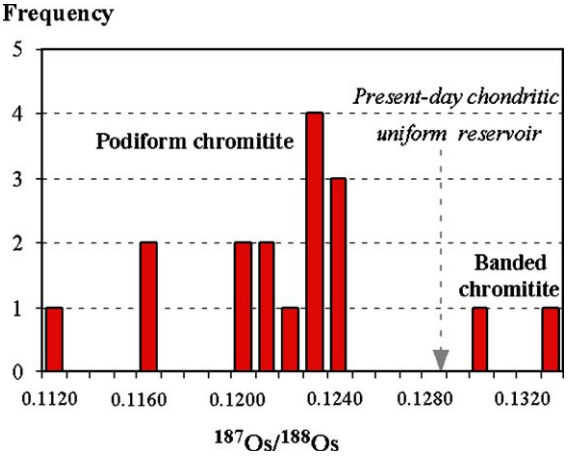

Fig. 5. Histogram of Os isotopic composition of Ru–Os sulfides from distinct chromitites at Kraubath, Austria.

6.1. Os isotope constraints for the sources of PGE mineralization and composition of the depleted mantle

Primary Ru–Os–Ir alloys and Ru–Os sulfides studied are considered to form early, either prior or contemporaneously to chromite formation (Augé and Johan, 1988; Melcher et al., 1997; Garuti et al., 1999). Textural and compositional data obtained for PGM

from podiform chromitite at Kraubath (Malitch et al., 2003b) indicates that the PGM were trapped as solids, either as individual laurites or Os–Ir alloys, or as polyphase assemblages containing PGE-alloys and laurite. The mechanism of laurite and IPGE alloy formation as inclusions in chromite is best explained by the "cluster" model proposed by Tredoux et al. (1995). During partial melting of the mantle source, the refractory PGE (IPGE) remain in the form of metallic clusters: a structure 3 to 100 atoms in size, in which all the atoms are connected to at least two other atoms by metal–metal bonds. According to this model (Tredoux et al., 1995), the clusters act as nuclei for the early-formed crystals of chromite, when favourable conditions are reached for chromite formation. The formation of a Ru–Os–Ir alloy or a Ru–Os sulfide will be controlled by availability of sulphur. In S-rich environments, sulfide minerals enclose the PGE clusters and associated ligands. In S-poor environments, the clusters remain free and coalesce to form alloys.

Equilibrium phase relationships of Ru–Os–Ir alloys at Kunar, based on the binary system diagrams Os–Ir, Os–Ru and Ir–Ru (Massalski, 1993), and the presence of a ruthenium trend in IPGE alloys (Fig. 4A) are indicative of high temperatures and pressures, which can only be reached under mantle conditions (Bird and Bassett, 1980). These refractory alloys are considered to be representative of depleted mantle material exemplified by mantle sections of ophiolites. The high temperature of formation of Ru–Os sulfides and IPGE alloys, which has been confirmed experimentally (Andrews and Brenan, 2002), implies that the Os isotopic compositions of Ru–Os sulfides and IPGE alloys should reflect that of the source region. Therefore, the low 'unradiogenic' $^{187}Os/^{188}Os$ values of the studied PGM clearly indicate a common chondritic or subchondritic mantle source for the PGE. Consequently, the PGE were derived from the mantle source without any significant crustal contribution of Os, and the $^{187}Os/^{188}Os$ values have not been changed by subsequent processes such as metamorphism and surface transport, sedimentation and weathering during placer formation.

The Os isotope compositions of Ru–Os–Ir alloys at Kunar and laurite at Kraubath correspond to those estimated for the mantle peridotites, which are characterised by relatively low $^{187}Os/^{188}Os$ values as a result of their evolution in a low Re/Os environment (Shirey and Walker, 1998). However, the Os isotopic compositions of laurites, measured by N-TIMS and LA MC-ICP-MS, vary from that of whole-rock chromite concentrates and podiform chromitite at Kraubath and Hochgrössen (Meisel et al., 1997; Melcher and Meisel, unpublished data), which closely match either present-day depleted MOR mantle (DMM) or an enriched mantle source (e.g., 0.1239–0.1271 and 0.1329–0.2028, respectively). Osmium isotopic data obtained on chromite concentrates thus tend towards more radiogenic values, if compared to results for PGM obtained by N-TIMS and LA MC-ICP-MS studies. In order to explain this observation, one sample of podiform chromitite was disintegrated by the electric-pulse technique, which produces mineral concentrates with preserved grain boundaries. The disintegrated material was then split into five grain-size fractions (Melcher and Meisel, unpublished data). Although all fractions yielded comparable concentrations of Os (115 to 196 ppb), the less refractory PGE such as Pd (21–76 ppb), Pt (50–189 ppb) and especially Re (0.09–6.91 ppb) were strongly concentrated in the finest (<63 μm) fraction. The latter also yielded the most 'radiogenic' $^{187}Os/^{188}Os$ value (0.1661) compared to 0.123 in the most coarse grain fraction. Since the sample had been disintegrated using the electric-pulse technique, PGM originally enclosed in chromite were not liberated into the fine fraction, and thus were the major contributor to the whole rock PGE budget. In coarse chromite grains, the number of primary Ru–Os sulfides with 'unradiogenic' $^{187}Os/^{188}Os$ values can be high, resulting in a relatively 'unradiogenic' initial value. However, in the fine fractions, the contribution of primary PGM enclosed in primary chromite grains is outweighed by the contribution of interstitial phases. These may be either primary or secondary Re-containing minerals causing ingrowth of 'radiogenic' ^{187}Os, or some PGM with a more 'radiogenic' composition that could have crystallized from interstitial melt. The latter option has not been verified by our LA MC-ICP-MS studies.

'Unradiogenic' $^{187}Os/^{188}Os$ values of laurite and ruarsite from the Eastern Alpine podiform chromitites (Malitch et al., 2003a; this study) clearly match those of detrital Ru–Os–Ir alloys from the Kunar Complex. Furthermore, these PGM, which are representative of Proterozoic dunite–harzburgite complexes, have a range of subchondritic $^{187}Os/^{188}Os$ values that is almost indistinguishable from that of detrital Ru–Os–Ir

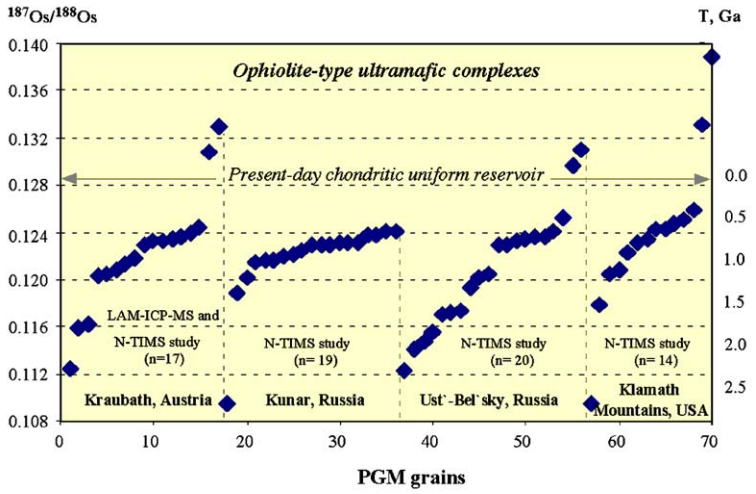

Fig. 6. Os isotopic composition of PGM from ophiolite-type ultramafic complexes. N-TIMS and LA MC-ICP-MS data for Kraubath and Kunar—this study. N-TIMS data are from Rudashevsky et al. (1999) for Ust'-Bel'sky PGM and from Meibom and Frei (2002) for Klamath Mountains PGM.

alloys derived from Mesozoic dunite–harzburgite complexes (e.g., the Ust'-Bel'sky Complex, Far East, Russia, and the Klamath Mountains, California and Oregon, USA, Fig. 6, 0.1094–0.1259, $n=64$). Therefore, substantial Os isotope heterogeneity of 'unradiogenic' $^{187}Os/^{188}Os$ values is proposed to be typical of PGM from the mantle section of an ophiolite.

In contrast to PGM with subchondritic $^{187}Os/^{188}Os$ signatures, erlichmanite and laurite from banded chromitite within the Moho transition zone at Kraubath show high $^{187}Os/^{188}Os$ values (0.13080 ± 0.00011 to 0.13212 ± 0.00065), indicative of a suprachondritic source of PGE (Figs. 5 and 6). This feature may be interpreted as evidence of a 'radiogenic' crustal component, which was introduced during a subduction-related event or an indication of an enriched mantle source. Consequently, suprachondritic $^{187}Os/^{188}Os$ values (>0.12863), which also have been detected in detrital Os–Ir alloys grains (Fig. 6) may indicate derivation from a distinct source other than residual dunite–harzburgite sequences of an ophiolite complex. As evident from the Ru–Os sulfides from banded chromitite at Kraubath, one of the bedrock sources for the highly 'radiogenic' sulfides can be the Moho transition zone of an ophiolite. Osmium isotopic evidence supports a distinct origin for podiform and banded chromitites, proposed on the basis of geological, geochemical and mineralogical data (Malitch et al., 2003b).

The high degree of Os isotopic heterogeneity identified implies that only comprehensive sets of Os isotope data obtained from geologically well-constrained samples (e.g., PGM, chromite, chromitite, etc.) can provide a valid understanding of Os isotopic behavior in the depleted upper mantle. Therefore, conclusions based only on Os isotope data for detrital Os–Ir alloy grains from museum samples (Meibom et al., 2002) or deduced from a restricted number of Os isotope analyses of chromite separates from a particular ophiolite (Walker et al., 2002) must be treated with caution. For instance, Meibom et al. (2002) suggested that long-lived $^{187}Os/^{188}Os$ heterogeneity observed in Os–Ir alloys is due to the presence of unradiogenic Os-rich mantle sulfides, which were capable of equilibrating with more radiogenic Os in the melt. This assumption, however, is not based on proven facts. The PGM studied by Meibom et al. (2002) were Os–Ir alloys and no Os isotope data for Os-rich sulfides were presented. All the factors mentioned above imply that once extensive Os isotopic data on bedrock PGM from ophiolites of different age (i.e., Proterozoic, Paleozoic, Mesozoic, Cenozoic) become available a more precise Os isotopic estimate of the composition of the depleted upper mantle could be proposed.

6.2. Os isotope constraints for timing of mantle melting and geodynamic implications

With rare exceptions, most ophiolites world-wide are considered to be younger than 1 Ga. Their ages of formation show distinct peaks in the Late Proterozoic (Late Riphean), Cambro-Ordovician and Jurassic–Cretaceous (Abbate et al., 1985). The Kunar dunite–harzburgite massif, part of Chelyuskin ophiolite Belt in the Taimyr Peninsula, has been documented by several workers (e.g., Zalyaleev and Bezzubtsev, 1975; Bezzubtsev et al., 1986). The Chelyuskin ophiolite is correlated with coeval ophiolites of other Arctic regions that mark opening of the Paleo-Pacific Ocean and the breakup of the Neoproterozoic supercontinent Rodinia between 700 and 590 Ma as proposed by Powell et al. (1994). In contrast, Dobretsov et al. (1995) have suggested the same event occurred between 900 and 700 Ma. The obtained Os isotope results are consistent with a Late Proterozoic age for the formation of the Cheluyuskin ophiolite (~ 665 Ma), which is older than the time of its emplacement into crustal levels (~ 600 Ma, Vernikovsky and Vernikovskaya, 2001). Osmium isotope systematics suggest that melt depletion events, recorded by 'unradiogenic' $^{187}Os/^{188}Os$, at Kunar and certain other peridotite occurrences world-wide (e.g., Parkinson et al., 1998; Snow and Schmidt, 1999; Malitch et al., 2002; Fig. 6) are older than the time of their emplacement into crustal levels. This observation is similar to the phenomenon recorded by Re–Os isotopes in sulfide inclusions in diamonds (Spetsius et al., 2002). On the other hand, statistical data on the ages of Ru–Os–Ir alloys at Kunar (this study) and the Urals, Russia (Kostoyanov et al., unpublished data), show several stages of PGM formation with an average cycle of 150–200 Ma. This variability is likely to be due to discrete mantle melting events, which are probably controlled by deep-geodynamic processes (Dobretsov and Kirdyashkin, 1998).

Based on osmium isotopic compositions of laurites, modal age estimates for the formation of the ultramafic protoliths in the Eastern Alps range from 2248 to 601 Ma (Table 4). This suggests that Ru–Os sulfides within refractory chromite can indeed remain isolated from Os-isotopic equilibrium under mantle conditions, implying that residual mantle sections of ophiolites can preserve compositional heterogeneities for about 1.6 Ga. The robustness of the Os-isotope system for Ru–Os–Ir alloys and Ru–Os sulfides has been documented at Witwatersrand (Malitch et al., 2000) and the Eastern Alps (Malitch et al., 2003a). So far, no evidence for resetting of the Os-isotopic system of these minerals has been observed. Furthermore, it is highly unlikely that Ru–Os sulfides found as euhedral inclusions in chromite may interact with radiogenic osmium since these PGM are protected by resistant chromite. Therefore, $^{187}Os/^{188}Os$ model ages are indicative of the existence of a Precambrian ultramafic parent protolith, which most likely formed during the Late Proterozoic.

The considerable scatter of the chondritic to subchondritic $^{187}Os/^{188}Os$ values of laurite from podiform chromitite at Kraubath (0.11249–0.12437, $n = 15$) and detrital Ru–Os–Ir alloys at Kunar (0.1094–0.1239, $n = 19$) provides isotopic evidence for locally restricted but temporally extended periods of PGM formation in the depleted upper mantle. The Os isotopic compositions of these PGM indicates that they record much older melting events than would be expected from a single-melting model of undepleted mantle. One of the explanations of this phenomenon is that after their formation, PGM remained isolated from the convecting upper mantle. In this case, ultramafic rocks of the Kunar and Kraubath massifs are not simple residues after partial melting at a mid-ocean ridge system or evolved back-arc in the Late Proterozoic. Instead, they may represent a mixture of (1) refractory isolated blocks that retain much older ages and (2) ultramafic rocks formed during a partial melting episode in the Late Proterozoic (~ 650 and ~ 780 Ma, respectively). A similar scenario has been advocated by Parkinson et al. (1998), and Snow and Schmidt (1999) for the Izu-Bonina-Mariana and Zabargad peridotites, respectively. Furthermore, Os isotope model ages of PGM at Kraubath are older than the time of formation of orthopyroxenite (~ 550 Ma) implying that subduction zones indeed may represent graveyards for ancient oceanic lithosphere as proposed by Parkinson et al. (1998).

The preferred interpretation for the wide range of subchondritic $^{187}Os/^{188}Os$ values for primary PGM (e.g., laurite and Ru–Os–Ir alloys) derived from the dunite–harzburgite complexes worldwide (Fig. 6) is consistent with a model, in which a prolonged history of melting events of parent ultramafic source rocks took place in the mantle. This accords well with the

conclusion that "the Os isotopic system of PGM records multiple events in the chemical differentiation history of the mantle (Carlson, 2002)". On the other hand, another interpretation could be that the mantle source, from which PGM derived, was much less radiogenic than presently assumed. In this scenario, Os isotope heterogeneity might also reflect the effect of variable degrees of partial melting of this mantle source. Finally, the origin of this heterogeneity may be also attributed to the presence of subcontinental lithospheric mantle (SCLM), characterized by unradiogenic $^{187}Os/^{188}Os$ values [i.e., <0.1220 (Handler et al., 1997)], which has lately been incorporated into the asthenospheric mantle with more radiogenic $^{187}Os/^{188}Os$ values (0.1220–0.1230; Snow and Reisberg, 1995; Shirey and Walker, 1998)]. However, once Os isotopic data on bedrock PGM from Phanerozoic ophiolites become available, a more plausible explanation can be developed.

7. Conclusions

1. For the first time, a combined compositional study (EMPA, N-TIMS and LA MC-ICP-MS) focuses on the Os isotopic system of primary Ru–Os sulfides and Ru–Os–Ir alloys from two Neoproterozoic ophiolite-type ultramafic massifs (i.e., Kunar in Northern Taimyr, Russia, and Kraubath in Eastern Alps, Austria). A wide scatter of osmium isotope compositions of PGM (i.e., $^{187}Os/^{188}Os$ varies in the range 0.10940–0.13210) along with two contrasting sources of PGE-mineralization have been identified.
2. Laurites from podiform chromitite at Kraubath and detrital Ru–Os–Ir alloys at Kunar are characterized by 'unradiogenic' $^{187}Os/^{188}Os$ values, indicative of a subchondritic mantle source of PGE. These values yield a very wide range of $^{187}Os/^{188}Os$ (0.10940 to 0.12437). The 'unradiogenic' $^{187}Os/^{188}Os$ values combined with the documented high degree of Os isotopic heterogeneity is considered a feature typical of the PGM from the mantle section of an ophiolite.
3. Ru–Os sulfides (laurite and erlichmanite) from banded chromitite at Kraubath, which occur immediately above the typical mantle section with podiform chromitite, have 'radiogenic' $^{187}Os/^{188}Os$ (0.1308 to 0.1321) values, indicative of a suprachondritic source of PGE. Consequently, suprachondritic $^{187}Os/^{188}Os$ values (>0.12863), which also have been subordinately detected in detrital PGM grains from ophiolites, might indicate a derivation from the transition zone or crustal sequence within an ophiolite.
4. Calculated $^{187}Os/^{188}Os$ model ages of laurite and Ru–Os–Ir alloys, assuming a chondritic uniform reservoir, range from 2669 to 601 Ma. Therefore, they likely indicate the existence of Precambrian ultramafic parent protoliths. The range of model ages for PGM at Kunar (2669–639 Ma) is similar to that of PGM from Kraubath (2248–601 Ma). The Os isotopic system of PGM thus unequivocally recorded temporally extended melting events in the Eastern Alpine and Chelyuskin parent ultramafic protoliths, indicating that ophiolites in the Proterozoic have a more complex geological history than it is frequently assumed.
5. The Os isotope results show that the Re–Os system in PGM has remained closed and unchanged from the time of formation of the PGM until now, despite later thermal events affecting both massifs. The long-lived osmium isotope heterogeneity obtained implies that only comprehensive sets of Os isotope data can provide a valid understanding of Os isotopic behaviour in the depleted upper mantle. Therefore, inferences drawn from a restricted number of Os isotope analyses, especially those obtained on whole rocks, should be treated with caution. Finally, it is suggested that the Os isotopic composition of PGM can be employed to test the validity of various petrological models.

Acknowledgements

This is a contribution for IGCP Project 479. The financial support by (1) the Committee for Geology and Utilization of Natural Resources of Taimyr region ("Taimyrkomprirodresursy", Noril'sk, Russia) (Project 98/6-H to K.N.M.), (2) the Austrian Science Fund (FWF Project M601-CHE to K.N.M.), and (3) Mining University of Leoben (Guest Professorship to K.N.M.) is gratefully acknowledged. I am indebted to Mikhail M. Goncharov and Oleg N. Simonov for logistic support during the field work, to Stephan A.

Junk, Vladimir V. Knauf, Anatoly I. Kostoyanov, Frank Melcher, Helmut Mühlhans, Ernst Pernicka, Nikolai S. Rudashevsky, Eugen F. Stumpfl and Oskar A.R. Thalhammer for valuable analytical assistance and stimulating discussions during long-lasting cooperation. I am very grateful to Alistair McCready for improving the English in the revised draft of the manuscript. This paper has benefitted from constructive reviews by Olivier Alard, Thierry Auge, John M. Bird and an unidentified reviewer. Careful handling and editorial input by Guest Editors Olivier Alard and Laurie Reisberg are greatly appreciated. **[RR]**

References

Abbate, E., Bortolotti, V., Passerini, P., Principi, G., 1985. The rhythm of Phanerozoic ophiolites. Ofioliti 10, 109–138.

Alard, O., Luguet, A., Lorand, J.-P., Pearson, N.J., Griffin, W.L., O'Reilly, S.Y., 2001. Extreme Os isotopic heterogeneity in magmatic sulfides of oceanic peridotites. Journal of Conference Abstracts, vol. 6 (1). Cambridge Publications, Cambridge, UK, p. 451.

Alard, O., Griffin, W.L., Pearson, N.J., Lorand, J.-P., O'Reilly, S.Y., 2002. New insights into the Re–Os systematics of sub-continental lithospheric mantle from in situ analysis of sulphides. Earth Planet. Sci. Lett. 203, 651–663.

Allègre, C.J., Luck, J.-M., 1980. Osmium isotopes as petrogenetic and geological tracers. Earth Planet. Sci. Lett. 48, 148–154.

Andrews, D.R.A., Brenan, J.M., 2002. Phase-equilibrium constraints on the magmatic origin of laurite+Ru–Os–Ir alloy. Can. Mineral. 40, 1705–1716.

Augé, T., Johan, Z., 1988. Comparative study of chromite deposits from Troodos, Vourinos, North Oman and New Caledonia ophiolites. In: Boissonnas, J., Omenetto, P. (Eds.), Mineral Deposits within the European Community. Society for Geology Applied to Mineral Deposits Spec. Publ., vol. 6. Springer-Verlag, Berlin-Heidelberg, Germany-New York, USA, pp. 267–288.

Bezzubtsev, V.V., Zalyaleev R.S. and Sakovitch, A.B., 1986. 1:500 000 Geological map of Gorny Taimyr, explanatory note. Krasnoyarsk, 177 pp. (in Russ.).

Bird, J.M., Bassett, W.A., 1980. Evidence of a deep mantle history in terrestrial osmium–iridium–ruthenium alloys. J. Geophys. Res. 85, 2012–2019.

Burton, K.W., Schiano, P., Birck, J.-L., Allègre, C.J., 1999. Osmium isotope disequilibrium between mantle minerals in a spinel-lherzolite. Earth Planet. Sci. Lett. 172, 311–322.

Cabri, L.-J., Harris, D.C., Weiser, T.W., 1996. Mineralogy and distribution of platinum-group mineral (PGM) placer deposits of the world. Explor. Min. Geol. 5, 73–167.

Carlson, R.W., 2002. Osmium remembers. Science 296, 475–477.

Cassard, D., Nicolas, A., Rabinovitch, M., Moutte, J., Leblanc, M., Prinzhofer, A., 1981. Structural classification of chromite pods in southern New Caledonia. Econ. Geol. 76, 805–831.

Chen, J.H., Papanastassiou, D.A., Wasserburg, G.J., 1998. Re–Os systematics in chondrites and the fractionation of the platinum-group elements in the early solar system. Geochim. Cosmochim. Acta 62, 3379–3392.

Creaser, R.A., Papanastassiou, D.A., Wasserburg, G.J., 1991. Negative thermal ion mass spectrometry of osmium, rhenium, and iridium. Geochim. Cosmochim. Acta 55, 397–401.

Dobretsov, N.L., Kirdyashkin, A.G., 1998. Deep-Level Geodynamics. Swets and Zeitlinger, Rotterdam, Netherlands. 328 pp.

Dobretsov, N.L., Berzin, N.A., Buslov, M.M., 1995. Opening and tectonic evolution of the Paleo-Asian ocean. Int. Geol. Rev. 37, 335–360.

Faryad, S.W., Melcher, F., Hoinkes, G., Puhl, J., Meisel, T., Frank, W., 2002. Relics of eclogite facies metamorphism in the Austoalpine basement, Hochgrössen (Speik Complex), Austria. Mineral. Petrol. 74, 49–73.

Garuti, G., Zaccarini, F., Moloshag, V., Alimov, V., 1999. Platinum-group minerals as indicators of sulfur fugacity in ophiolitic upper mantle: an example from chromitites of the Rai-Iz ultramafic complex, Polar Urals, Russia. Can. Mineral. 37, 1099–1115.

Handler, M.R., Bennett, V.C., Esat, T.M., 1997. The persistence of off-cratonic lithospheric mantle: Os isotopic systematics of variably metasomatised southeast Australian xenoliths. Earth Planet. Sci. Lett. 151, 61–75.

Harris, D.C., Cabri, L.J., 1991. Nomenclature of platinum-group-element alloys: review and revision. Can. Mineral. 29, 231–237.

Hart, S.R., Ravizza, G.E., 1996. Os partitioning between phases in lherzolite and basalt. In: Basu, A., Hart, S.R. (Eds.), Earth Processes: Reading the Isotopic CodeGeophys. Monogr. Ser., vol. 95. AGU, Washington, USA, pp. 123–134.

Hattori, K., 2002. A review of rhenium–osmium isotope geochemistry of platinum-group minerals and platinum mineralization. In: Cabri, L.J. (Ed.), The Geology, Geochemistry, Mineralogy and Mineral Beneficiation of Platinum-Group Elements. Canadian Institute of Mining, Metallurgy and Petroleum, Spec., vol. 54, pp. 251–271.

Hattori, K., Hart, S.R., 1991. Osmium–isotope ratios of platinum-group minerals associated with ultramafic intrusions: Os-isotopic evolution of the oceanic mantle. Earth Planet. Sci. Lett. 107, 499–514.

Hattori, K., Burgath, K.-P., Hart, S.R., 1992. Os-isotope study of platinum-group minerals in chromitites in Alpine-type ultramafic intrusions and the associated placers in Borneo. Mineral. Mag. 56, 157–164.

Hirata, T., Hattori, M., Tanaka, T., 1998. In-situ osmium isotope ratio analyses of iridosmines by laser ablation-multiple collector-inductively coupled plasma mass spectrometry. Chem. Geol. 144, 269–280.

Junk, S.A., 2001. Ancient artefacts and modern analytical techniques—usefulness of laser ablation ICPMS demonstrated with ancient gold coins. Nucl. Instrum. Methods Phys. Res., B Beam Interact. Mater. Atoms 181, 723–727.

Kostoyanov, A.I., Manoilov, V.V., Efis, Yu.M., Rodionov, M.V., 2000. A mass spectrometer complex for measuring the isotopic composition of the difficult to ionize metals. Instrum. Exp. Tech. 43, 91–93.

Luck, J.-M., Allègre, C.J., 1991. Osmium isotopes in ophiolites. Earth Planet. Sci. Lett. 107, 406–415.

Malitch, K.N., 1999. Platinum-Group Elements in Clinopyroxenite–Dunite Massifs of the Eastern Siberia (Geochemistry, Mineralogy, and Genesis). Saint Petersburg Cartographic Factory VSEGEI Press, St. Petersburg, Russia. 296 pp., in Russ.

Malitch, K.N., Kostoyanov, A.I., Merkle, R.K.W., 2000. Mineral composition and osmium isotopes of PGE-mineralization of Eastern Witwatersrand (South Africa). Geologiya Rudnykh Mestorozhdenii 42, 281–295 (in Russ.).

Malitch, K.N., Melcher, F., Mühlhans, H., 2001. Palladium and gold mineralization in podiform chromitite at Kraubath, Austria. Mineral. Petrol. 73, 247–277.

Malitch, K.N., Augé, T., Badanina, I.Yu., Goncharov, M.M., Junk, S.A., Pernicka, E., 2002. Os-rich nuggets from Au-PGE placers of the Maimecha-Kotui Province, Russia: a multi-disciplinary study. Mineral. Petrol. 76, 121–148.

Malitch, K.N., Junk, S.A., Thalhammer, O.A.R., Melcher, F., Knauf, V.V., Pernicka, E., Stumpfl, E.F., 2003a. Laurite and ruarsite from podiform chromitites at Kraubath and Hochgrössen, Austria: new insights from osmium isotopes. Can. Mineral. 41, 331–352.

Malitch, K.N., Thalhammer, O.A.R., Knauf, V.V., Melcher, F., 2003b. Diversity of platinum-group mineral assemblages in banded and podiform chromitite from the Kraubath ultramafic massif, Austria: evidence for an ophiolitic transition zone? Miner. Depos. 38, 282–297.

Massalski, T.B. (Ed.), 1993. Binary Alloy Phase Diagrams. Amer. Soc. Metals Metals Park, Ohio. 2224 pp.

Meibom, A., Frei, R., 2002. Evidence for an ancient osmium isotopic reservoir in Earth. Science 296, 516–518.

Meibom, A., Sleep, N.H., Chamberlain, C.P., Coleman, R.G., Frei, R., Hren, M.T., Wooden, J.L., 2002. Re–Os isotopic evidence for long-lived heterogeneity and equilibration processes in the Earth's upper mantle. Nature 419, 705–708.

Meisel, T., Melcher, F., Tomascak, P., Dingeldey, C., Koller, F., 1997. Re–Os isotopes in orogenic peridotite massifs in the Eastern Alps, Austria. Chem. Geol. 143, 217–229.

Meisel, T., Walker, R.J., Irving, A.J., Lorand, J.-P., 2001. Osmium isotopic composition of mantle xenoliths: a global perspective. Geochim. Cosmochim. Acta 65, 1311–1323.

Melcher, F., Grum, W., Simon, G., Thalhammer, T.V., Stumpfl, E.F., 1997. Petrogenesis of the ophiolitic giant chromite deposits of Kempirsai, Kazakhstan: a study of solid and fluid inclusions in chromite. J. Petrol. 38, 1419–1458.

Melcher, F., Meisel, T., Puhl, J., Koller, F., 2002. Petrogenesis and geotectonic setting of ultramafic rocks in the Eastern Alps: constraints from geochemistry. Lithos 65, 69–112.

Neubauer, F., Frisch, W., Schmerold, R., Schlöser, H., 1989. Metamorphosed and dismembered ophiolite suits in the basement units of the Eastern Alps. Tectonophysics 164, 49–62.

Ohnenstetter, M., Johan, Z., Cocherie, A., Fouillac, A.M., Guerrot, C., Ohnenstetter, D., Chaussidon, M., Rouer, O., Makovicky, E., Makovicky, M., Rose-Hansen, J., Karup-Möller, S., Vaughan, D., Turner, G., Pattrick, R.A.D., Gize, A.P., Lyon, I., McDonald, I., 1999. New exploration methods for platinum and rhodium deposits poor in base-metal sulphides—NEXTRIM. Trans.-Inst. Min. Metall., B, Appl. Earth Sci. 108, B119–B150.

Parkinson, I.J., Hawkesworth, C.J., Cohen, A.S., 1998. Ancient mantle in a modern arc: osmium isotopes in Izu-Bonin-Mariana forearc peridotites. Science 281, 2011–2013.

Powell, C.McA., Preiss, W.V., Gatehouse, C.G., Krapez, B., Li, Z.X., 1994. South Australian record of a Rodinian epicontinental basin and its mid-Neoproterozoic breakup (~ 700 Ma) to form the Paleo-Pacific Ocean. Tectonophysics 237, 113–140.

Rosman, K.J., Taylor, P.D.P., 1998. Isotopic composition of the elements 1997. Pure Appl. Chem. 70, 217–235.

Rudashevsky, N.S., Kostoyanov, A.I., Rudashevsky, V.N., 1999. Mineralogical and isotope evidences of origin of the Alpine-type massifs (the Ust'-Bel'sky massif, Koryak Highland, as an example). Zap. Vseross. Mineral. Obshchestva 128, 11–28 (in Russ.).

Shirey, S.B., Walker, R.J., 1998. The Re–Os isotope system in cosmochemistry and high-temperature geochemistry. Annu. Rev. Earth Planet. Sci. 26, 423–500.

Smoliar, M.I., Walker, R.J., Morgan, J.W., 1996. Re–Os ages of group IIA, IIIA, IVA, and IVB meteorites. Science 271, 1099–1102.

Snow, J.E., Reisberg, L., 1995. Os isotopic systematics of the MORB mantle: results from altered abyssal peridotites. Earth Planet. Sci. Lett. 136, 723–733.

Snow, J.E., Schmidt, G., 1999. Proterozoic melting in the northern peridotite massif, Zabargad island: Os isotopic evidence. Terra Nova 11, 45–50.

Spetsius, Z.V., Belousova, E.A., Griffin, W.L., O'Reilly, S.Y., Pearson, N.J., 2002. Archean sulfide inclusions in Paleozoic zircon megacrysts from the Mir kimberlite, Yakutia: implications for the dating of diamonds. Earth Planet. Sci. Lett. 199, 111–126.

Tredoux, M., Lindsay, N.M., Davies, G., McDonald, I., 1995. The fractionation of platinum-group elements in magmatic systems, with the suggestion of a novel causal mechanism. S. Afr. J. Geol. 98, 157–167.

Tsuru, A., Walker, R.J., Kontinen, A., Peltonen, P., Hanski, E., 2000. Re–Os isotopic systematics of the 1.95 Ga Jormua ophiolite complex, northeastern Finland. Chem. Geol. 164, 123–141.

Tuttas, D., 1992. The measurement of osmium isotope ratios using negative thermal ionization. Appl. News 1, 1–20.

Vernikovsky, V.A., Vernikovskaya, A.E., 2001. Central Taimyr accretionary belt (Arctic Asia): Meso-Neoproterozoic tectonic evolution and Rodinia breakup. Precambrian Res. 110, 127–141.

Walker, R.J., Hanski, E., Vuollo, J., Liipo, J., 1996. The Os isotopic composition of Proterozoic upper mantle: evidence from the Outokumpu ophiolite, Finland. Earth Planet. Sci. Lett. 141, 161–173.

Walker, R.J., Prichard, H.M., Ishiwatari, A., Pimentel, M., 2002. The osmium isotopic composition of convecting upper mantle deduced from ophiolite chromites. Geochim. Cosmochim. Acta 66, 329–345.

Yin, Q., Jagoutz, E., Palme, H., Wanke, H., 1996. NUR—a possible proxy for CHUR reference for Re–Os system derived from $^{187}Os/^{188}Os$ ratio of the Allende CAI. Abstracts. Lunar and Planetary Science Conference. XXVII. Lunar and Planetary Institute, Houston, Texas, vol. 3, pp. 1475–1476.

Zalyaleev, R.Sh., Bezzubtsev, V.V., 1975. Chelyuskin ultramafic Belt. Geol. Geofiz. 16, 132–133 (in Russ.).